Statistical Cluster-QSO Weak Lensing in the Sloan Digital Sky Survey

Zhong-Lue Wen[1], Yan-Bin Yang[1], Xu Zhou[1], Qi-Rong Yuan[2] and Jun Ma[1]

[1] National Astronomical Observatories, Chinese Academy of Sciences, Beijing 100012
zlwen@vega.bac.pku.edu.cn
[2] Department of Physics, Nanjing Normal University, Nanjing 210097

Abstract We investigate the cross-correlation between galaxy clusters and QSOs using Sloan Digital Sky Survey (SDSS) DR4 $\sim 5000 \deg^2$ data. With photometric redshifts of galaxies, we select galaxy clusters based on the local projected densities of LRGs brighter than $M_{r'} = -22$. The QSOs are from the main sample of SDSS QSO spectroscopic survey to $i' = 19$. A significant positive correlation is found between the clusters and QSOs. Under the assumption that the signal is caused by gravitational lensing, we fit the signal with singular isothermal sphere (SIS) model and NFW profile halo model. The velocity dispersion $\sigma_v = 766 \mathrm{~km~s^{-1}}$ is derived for the best-fit of SIS model. Best-fit for the NFW model requires the dark matter halo mass within $1.5~h^{-1}$ Mpc to be $4.6 \times 10^{14}~h^{-1}~M_\odot$. The mass parameter $\Omega_{\rm cl}$ of the cluster sample is deduced as 0.077 with the SIS model and 0.083 with the NFW model. Our results of $\Omega_{\rm cl}$ are smaller than those given by Croom & Shanks and by Myers et al.

Key words: cosmology: observations – galaxies: clusters: general – quasars: general – gravitational lensing

1 INTRODUCTION

Foreground high density structures could introduce significant gravitational lensing effect on background sources (Schneider et al. 1992; Bartelmann & Schneider 1992, 1993; Wu & Han 1995; Fan & Chiueh 2000; Benitez et al. 2001; Gaztañaga 2003; Tang & Zhang 2005). The studies on gravitational lensing give us further understanding of the hierarchical structure formation (e.g., Maoz & Rix 1993; Brainerd et al. 1996; Griffiths et al. 1996) and constrain the abundance of compact objects in the universe (Schneider 1993). Gravitational lensing also provides new measurement of the cosmological parameters, such as σ_8, Ω_m and galaxy bias b (Hoekstra et al. 2001a, b; Contaldi et al. 2003; Hoekstra 2003).

Weak gravitational lensing affects the observed density of background sources in two related ways. First, sources are magnified, resulting in more fainter sources being observed in a magnitude-limited survey. Secondly, spatial scale is also magnified, causing a dilution of the observed density. Theoretically, the observed density depends on the slope of source number-magnitude relation (Schneider et al. 1992). It can be written in the form $n'(m) = n_0(m)\mu^{2.5\beta - 1}$, where $n_0(m)$ is the intrinsic source density, μ is the magnification factor, and β is the source number-magnitude slope defined as $\beta = d \log n_0/dm$. As a result, the lensing effect will lead to an enhancement for $\beta > 0.4$, and a deficit for $\beta < 0.4$. The density does not change for the critical value $\beta = 0.4$.

Since the last two decades, QSOs have been used as background sources in the study of weak gravitational lensing. This is because most QSOs are distributed at high redshifts, and they can be easily detected in optical (e.g., 2QZ, SDSS surveys) and radio (e.g., FIRST, CLASS surveys) bands due to their high luminosities. Many authors have investigated the cross-correlation between galaxies/clusters and background

QSOs. With radio-selected QSOs, positive correlations have been found (Seldner & Peebles 1979; Chu & Zhu 1984; Fugmann 1988, 1990; Bartelmann & Schneider 1994; Bartsch et al. 1997; Norman & Impey 1999, 2001). With optical-selected QSOs, positive (Williams & Irwin 1998), negative (Boyle et al. 1988; Benítez et al. 2001), and null (Martínez et al. 1999) correlations were found. Recently, Gaztañaga (2003) reported a positive galaxy-QSO cross-correlation using bright QSOs ($i' < 18.8$) from the SDSS QSO spectroscopic survey. Myers et al. (2003, 2005) detected negative correlations between 23 000 2QZ QSOs and foreground galaxies/clusters. Scranton et al. (2005), for the first time, detected positive, negative and null correlations in their analysis with SDSS 3800 $\deg^2$ photometric data containing $\sim 200\,000$ QSOs and 13 million galaxies.

Although these results are in qualitative agreement with the gravitational lensing effect, in most cases the amplitude of observed correlation is much higher than the theoretical prediction. Webster et al. (1988), Rodrigues-Williams & Hogan (1994), Williams & Irwin 1998, and Gaztañaga (2003) found positive correlations that are much stronger than the predictions. Croom & Shanks (1999) reanalyzed the result of Boyle et al. (1988) in term of gravitational lensing, showing that the amplitude requires the velocity dispersion in clusters to be 1286 $\mathrm{km\,s^{-1}}$, much higher than expected for the detected clusters. Similar problem also exists in Myers et al. (2003). Effort has been made to explain these disagreements. Wu & Fang (1996) considered environmental mass around the clusters, but contribution from environment remains insufficient to account for the observed correlations. Scranton et al. (2005) pointed out that the discrepancy is possibly due to systematic effects in the datasets. For example, the QSO sample is 20% contaminated by Galactic stars in Boyle et al. (1988), and the 2dF QSO survey is found to be less complete beyond $b_J = 20.2$ (Richards et al. 2005). However, how much these factors affect the result is still not very clear. In this paper, we address the question utilizing an unprecedented cluster sample and more complete QSO sample from the SDSS.

This paper is organized as follows: In Section 2 we describe the galaxy cluster selection algorithm. In Section 3 we describe the QSO sample used in this paper. In Section 4 we measure the two point angular cross-correlation function between the clusters and QSOs, and model the clusters as Singular Isothermal Spheres and NFW profile halos. We give a discussion in Section 5 and our conclusions in Section 6. Throughout this paper we adopt the ΛCDM cosmology model with $h = H_0/100\,\mathrm{km\,s^{-1}\,Mpc^{-1}} = 0.75$, $\Omega_m = 0.3$ and $\Omega_\Lambda = 0.7$.

2 GALAXY CLUSTER SELECTION

The Sloan Digital Sky Survey is a wide-field photometric and spectroscopic survey. It will provide five broad bands (u', g', r', i' and z') photometry over 10000 $\deg^2$ and follow-up spectroscopy of 10^6 galaxies (*http://www.sdss.org*). The spectroscopic galaxy survey observes galaxies with extinction-corrected Petrosian magnitude $r' < 17.77$ for the main sample (Strauss et al. 2002) and $r' < 19.5$ for the luminous red galaxy (LRG) sample (Eisenstein et al. 2001).

The galaxy sample is taken from SDSS DR4. With the five-band photometry, we estimate the photometric redshifts of galaxies down to $r' = 21$ using the technique of Yang et al. (2005). The algorithm can provide the photometric redshifts of galaxies with uncertainty $\sigma_z \sim 0.03$, on which we base to present galaxy cluster selection. The method of selection is similar to the classical one of Abell (1958) who selected clusters by counting the numbers of galaxies. With the photometric redshifts, we can count the numbers within a proper radius, excluding foreground and background galaxies. First, we select a sample of LRGs brighter than $M_{r'} = -22$ as cluster galaxy candidates. This is because LRGs have more precise photometric redshifts and they are more likely to be in the clusters. We note that spectroscopic redshifts are adopted as long as they are available and we apply the k-correction following Fukugita et al. (1995). Secondly, for each candidate at redshift z, we count the numbers of galaxies N within 0.5 h^{-1} Mpc and $z \pm 0.05$ based on the photometric redshifts. Thirdly, defining the density contrast of the environment of the LRG as $\delta = N/\langle N \rangle - 1$, where $\langle N \rangle$ is the mean counts with the same range at z, candidates with $\delta > 2$ are identified as cluster galaxies. Center of cluster is defined by the position of the LRG with the highest density contrast within 1 h^{-1} Mpc and $z \pm 0.05$, and the cluster redshift, by that of the central LRG. At high redshift, the mean density of galaxies is low, and a few counts could give a high ensity contrast. Some of these galaxies may not lie in the clusters. To reduce false selection, we eliminate those candidates with
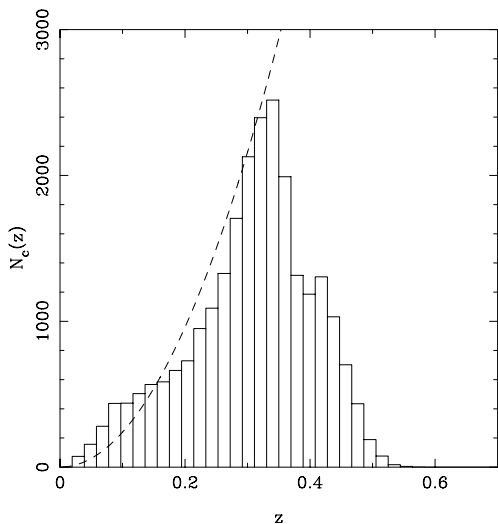
Fig. 1 Redshift distribution for the cluster sample. The dashed line represents the expected redshift distribution.
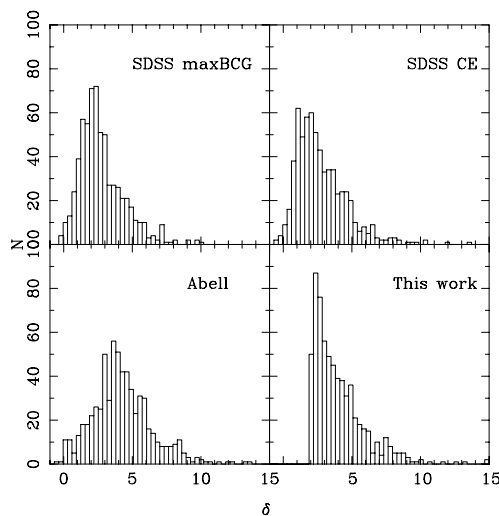
Fig. 2 Local projected density distribution for the selected clusters together with SDSS CE, maxBCG and Abell clusters containing selected LRGs. For comparison, the histograms are normalised to the same total.

galaxy counts less than $N = 12$. Figure 1 shows the redshift distribution of the cluster sample. [1] The dashed line represents the expected distribution.

Statistically, the value of δ reflects the richness of the cluster: richer clusters go with higher density contrasts. Figure 2 shows the histogram of δ for the clusters together with SDSS CE (Goto et al. 2002), SDSS maxBCG (Bahcall et al. 2003) and Abell (Abell 1958) cluster samples, in which clusters not containing the selected LRGs are excluded. There are 640 clusters in SDSS maxBCG sample (90%) contain the selected LRGs, and the histograms are normalized to this number. The figure shows that the median value of δ is ~ 2 for the SDSS CE and maxBCG samples, 3.5 for our sample and 4.5 for the Abell sample. For the following analysis, the velocity dispersion of the clusters is estimated. We adopt the velocity dispersions of the clusters given by Struble & Rood (1999) and we consider only those clusters that contain at least 10 known redshift members. Figure 3 plots the velocity dispersion against the density contrast: for clusters with $\delta \sim 3.5$ we find velocity dispersions in the range $400 - 600 \ \mathrm{km \ s^{-1}}$.

3 QSO SAMPLE

The SDSS imaging data reach a depth of $r' \sim 22.2$ for point sources (Abazajian et al. 2004). The QSO spectroscopic survey observes point objects down to a limiting PSF magnitude of $i' = 19.1$ for $z < 3$ QSOs and $i' = 20.2$ for high-z ($z > 3$) QSOs (Richards et al. 2002). Vanden Berk et al. (2005) have shown that the completeness of the selection algorithm is approximately 95%, and the overall completeness of the SDSS QSO survey is 89%. Figure 4 shows the redshift distribution of the QSO sample. Here, we restrict the sample to $0.6 < z < 2.3$ and exclude QSOs with redshift confidence parameter specobj.zConf < 0.7. The QSOs at lower redshift are also excluded to avoid overlap between clusters and QSOs. The upper limit is set because of the low completeness in the range $2.5 < z < 3$ where the quasar locus crosses the stellar locus (Richards et al. 2002). Figure 5 shows the QSOs' number-magnitude relation, which suggests that the SDSS QSO survey is complete to extinction-corrected $i' = 19$. The dashed line shows the power law fit between $17.5 < i' < 19$ with $\beta = 0.75$. Although the slope is larger at the brighter end, the QSOs there contribute only 5% to the total sample. Correction for data incompleteness gives $\beta = 0.78$, which is consistent with that of Richards et al. (2004) and Croom et al. (2004).

---

[1] The catalog is published as online data (*http://www.chjaa.org/2006_6_5.htm*).
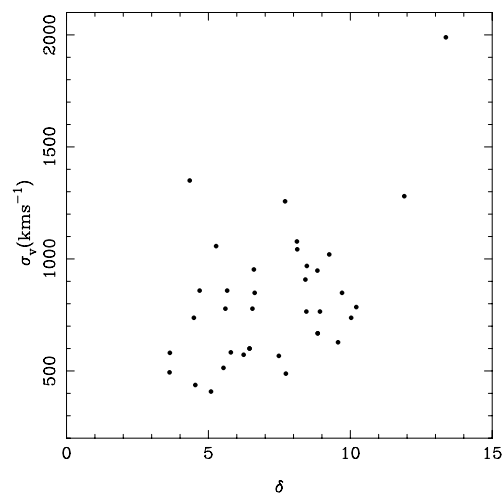
Fig. 3 Density contrast against velocity dispersion for 35 Abell clusters that contain at least 10 known redshift members.
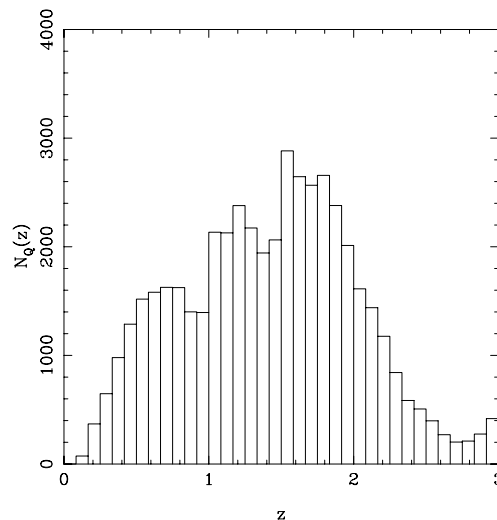
Fig. 4 Redshift distribution of the SDSS QSOs.
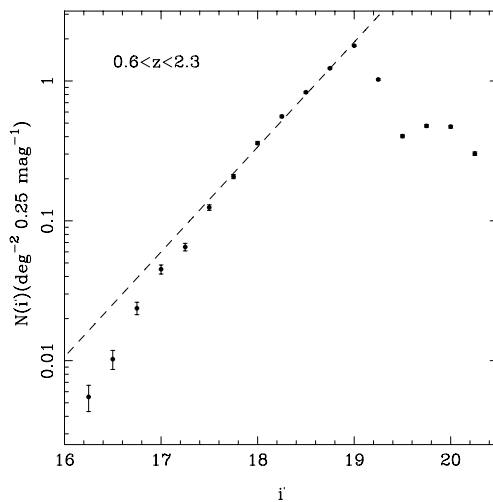
Fig. 5 Number-magnitude relation in i' for QSOs with $0.6 < z < 2.3$. The points are QSO number counts in 0.25 mag bins, with Poisson errors. The dashed line shows the power law fit with slope 0.75.

4 CROSS-CORRELATION MEASUREMENT

4.1 Weak Lensing Model

The hierarchical clustering model predicts that galaxy clusters are formed in the intersections of filaments. Mass accumulated in a rich cluster can reach $10^{15} M_\odot$. As the largest bound systems in the universe, galaxy clusters are the most likely objects that magnify background sources. Then, weak gravitational lensing can provide an independent way of obtaining the cluster mass distribution. According to the gravity theory, the bending angle of light passing through a cluster is (Young et al. 1980)

$$\alpha = \frac{4GM(b)}{bc^2} = \frac{D_s}{D_{ls}}(\theta - \theta_q), \tag{1}$$

where $M(b)$ is the projected mass within impact parameter b, D_s is the angular diameter distance of the source from the observer, D_{ls} is the angular diameter distance of the source from the lens, θ_q and θ are the angular distances of the lens to the source and to the image, respectively. The flux of sources will be magnified by a factor (Turner et al. 1984)

$$\mu(\theta) = \left| \frac{\theta}{\theta_q} \frac{d\theta}{d\theta_q} \right|. \tag{2}$$

The two point angular cross-correlation function $\omega_{cq}(\theta)$ is defined as the excess probability of finding a source at an angular distance from a given cluster:

$$\omega(\theta) \equiv \left\langle \frac{n'(m) - n_0(m)}{n_0(m)} \right\rangle = \mu(\theta)^{2.5\beta - 1} - 1. \tag{3}$$

Therefore, the observed correlation allows us to determine the mass distribution of a cluster. One general way is to assume a parameterized mass profile and we find the parameters that give the best fit to the observed correlation.

For simplicity, we assume that the clusters are isolated halos and ignore their shapes and substructures, and that the contribution to the ω_{cq} comes all from the considered central cluster while no contribution from the other clusters. The simplest model is that the cluster is considered as a singular isothermal sphere (SIS). The mass distribution is then given by

$$\rho(r) = \frac{\sigma_v^2}{2\pi G} \frac{1}{r^2}, \tag{4}$$

where σ_v is the velocity dispersion of the SIS. Another model adopted in this study is the NFW profile halo model provided by N-body simulations (Navarro et al. 1995, 1996, 1997):

$$\rho(r) = \frac{\rho_s}{\frac{r}{r_s}(1 + \frac{r}{r_s})^2}, \tag{5}$$

where r_s and ρ_s are the characteristic scale and density of the halo, respectively, with r_s given by the relation (Maoz et al. 1997),

$$r_s = 300\left(\frac{M_{1.5}}{10^{15} M_\odot}\right)^\gamma h^{-1} \text{kpc}, \tag{6}$$

where $\gamma = 1/3$ is adopted. This model is thus reduced to a single parameter, the mass of halo within $1.5\, h^{-1}$ Mpc of the halo ($M_{1.5}$).

4.2 Model Fits

The two point angular cross-correlation between clusters and QSOs is measured by the excess probability of finding pairs of the two sources separated by angle θ above the probability expected for a random distribution (Peebles 1980; Myers et al. 2003)

$$\omega_{cq}(\theta) = \frac{DD(\theta) n_R}{DR(\theta) n_D} - 1, \tag{7}$$

where D refers to a data point (either a QSO or a galaxy cluster) and R refers to random sample. DD is the actual number of QSO-cluster pairs of a given separation and DR is the number of QSO-cluster pairs in a Poisson random distribution. The random catalog is simulated precisely for the same area as the selected clusters. The parameter n_R/n_D is the ratio of number of mock clusters to that of real clusters. We adopt $n_R/n_D = 10$ in our simulations. For each Poisson random sample, the correlation is computed. Errors are measured as the rms of the calculated correlations of 50 random samples.
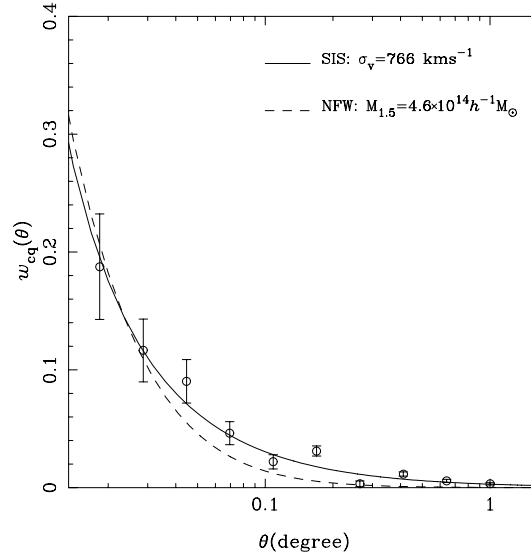
Fig. 6 Best-fit of the observed correlation with the SIS and NFW models. The SIS best fit is at velocity dispersion $\sigma_v = 766$ km s^{-1}; the NFW best fit is at dark matter halo mass within 1.5 h^{-1} Mpc equal to $4.6 \times 10^{14} h^{-1} M_\odot$.

Figure 6 displays the cluster-QSO two point angular cross-correlation (positive values shown). Based on the weak lensing model, we determine the best-fit SIS and NFW profile halo models by minimizing the χ^2 statistic. For the SIS, the best fit is at velocity $\sigma_v = 766 \pm 14$ km s^{-1}; for the NFW, at halo mass within 1.5 h^{-1} Mpc equal to $4.6 \pm 0.4 \times 10^{14} h^{-1} M_\odot$. When the corrected number-magnitude slope is used, these values decrease to $\sigma_v = 738$ km s^{-1} and $M_{1.5} = 4.3 \times 10^{14} h^{-1} M_\odot$.

4.3 Total Mass Estimation

From given mass or velocity dispersion of the individual clusters, we can express the total mass in clusters as a product of the space density of clusters and an average mass. Following the method of Croom & Shanks (1999), we derive the space density of the clusters to be $n = 5 \times 10^{-5} h^3$ Mpc^{-3} by integrating the proper volume to 0.35 and assuming that all clusters are detected to this redshift. The SIS model gives the mass parameter of the cluster sample

$$\Omega_{\rm cl} = 0.077 \Big(\frac{r}{1\ h^{-1}\ {\rm Mpc}}\Big)\Big(\frac{\sigma_v}{766\ {\rm km\,s^{-1}}}\Big)^2, \tag{8}$$

where r is the extent of the cross-correlation. We adopt the value $r = 1\ h^{-1}$ Mpc given by Croom & Shanks (1999) and Myers et al. (2003). The NFW model gives

$$\Omega_{\rm cl} = 0.083 \frac{M_{\rm NFW}}{4.6 \times 10^{14}\ h^{-1}\ M_\odot}. \tag{9}$$

The results show that $\Omega_{\rm cl} = 0.077 \pm 0.003$ for SIS and $\Omega_{\rm cl} = 0.083 \pm 0.06$ for NFW halo. Note we only take into account the errors of velocity dispersion and $M_{1.5}$. Other errors are difficult to estimate. The cluster selection based on photometric redshifts could lead to a redshift dependence of the space density. See Figure 1. Moreover, the presence of substructures in the clusters and the line-of-sight effect of environment would cause systematic errors.

5 DISCUSSION

Both SIS and NFW models give $\Omega_{\rm cl} \sim 0.08$, which is nearly three times larger than the observational value $\Omega_{\rm cl} = 0.028$ obtained by Fukugita et al. (1998). In our analysis, we model clusters as isolated halos.

$$w_{cc}(\theta) = 2.4 \times \theta^{-0.8}$$
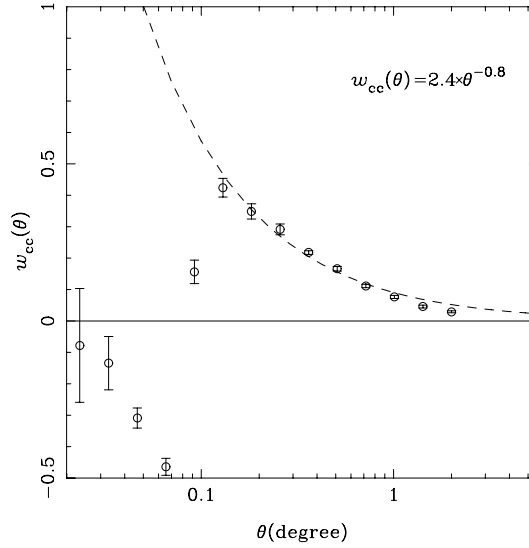
Fig. 7 Auto-correlation of clusters. The dashed line represents the power law fit in the form of $\omega_{cc} \sim \theta^{-0.8}$.

Table 1 Comparison with Previous Results

Authors	N_c	N_q	β	σ_v (km s^{-1})	$M_{1.5}$ ($h^{-1}\,M_\odot$)	Ω_{cl} SIS	NFW
Croom & Shanks (1999)	8442	2831 $B < 20.65$	0.29	1286	—	1.3	—
Myers et al. (2003)	1985	22417 $b_J < 20.85$	0.29	1156	1.2×10^{15}	1.06	1.3
This work	22505	23188 $i' < 19$	0.75	766	4.6×10^{14}	0.077	0.083

However, clusters are more complex than SIS and NFW models. There are substructures in the clusters and filaments connecting the clusters. It has been shown that galaxy filaments can comprise over 40% of the total mass at cluster radius between $4 - 6.5\,h^{-1}$ Mpc (Colberg et al. 1999; Cen & Ostriker 1999). Actually, the cross-correlation between cluster and large scale structure is still strong on the scale of $10\,h^{-1}$ Mpc (Mo et al. 1993). Such an environment of the clusters can contribute weak lensing signal (Wu & Fang 1996). Recently, Fan & Chiueh (2000) showed that the projected mass density of the environmental dark matter can be comparable to that of the cluster. On the other hand, the clusters are selected based on photometric redshifts of galaxies. Some of them can not be separated effectively if they are located along the same line-of-sight. Figure 7 shows the auto-correlation of clusters, the dashed line representing the power law $\omega_{cc} \sim \theta^{-0.8}$ fit. It suggests that the clusters can not be effectively separated below 0.1°. Assuming that the cluster auto-correlation function keeps the form of $\sim \theta^{-0.8}$ down to small scales, about 10% clusters are merged into the foreground or background ones. This also results in overestimates of the cluster mass.

Table 1 gives a comparison of our results with those of Croom & Shanks (1999) and Myers et al. (2003), who found negative correlations between clusters and QSOs. In both previous works, the QSOs came from deeper surveys with flat number-magnitude slopes and resulting in a mass parameter Ω_{cl} of ~ 1.0, much higher than Ω_m from the SDSS power spectrum analysis and WMAP (Tegmark et al. 2004), and more than 10 times higher than the value obtained here. The discrepancy may be mainly due to systematic errors in the space density of clusters. In both previous works, the redshifts of clusters were not determined and the space density was estimated following the galaxy distribution. However, the selection functions of galaxies

and clusters may be different, which would lead to large systematic errors in the estimation of the space density of clusters.

With the cluster selection and uncertainty of photometric redshift, we assume the number count of the LRGs to be one-fourth that of cluster members. The number of galaxies in the cluster sample corresponds to 15% of the total number of galaxies. Considering that the M/L ratio of cluster galaxies is twice as much as that of field galaxies (Colín et al. 1999), the expected Ω_m of the universe should be raised by a factor of 4.

6 CONCLUSIONS

From the Sloan wide-field photometric and spectroscopic survey, we selected galaxy clusters utilizing photometric redshifts of galaxies. After excluding foreground and background galaxies, we measured the local projected densities of LRGs. The clusters were identified based on LRGs with density contrast $\delta > 2$ and galaxy counts larger than 12. The algorithm selected more than 20,000 clusters from SDSS DR4 $\sim 5000 \deg^2$, with expected velocity dispersion $\sim 400 - 600$ km s^{-1} and space density $n = 5 \times 10^{-5}$ h^3 Mpc^{-3}.

We measured the two point angular cross-correlation between these clusters and SDSS bright QSOs ($i' < 19$), and found significant positive correlation. Because the slope of number-magnitude relation is steep for the QSOs, gravitational lensing is suggested as the physical process to produce the signal. We model clusters as singular isothermal spheres (SIS) and NFW profile halos. The best-fit for the SIS model requires the velocity dispersion to be 766 km s^{-1}, and for NFW model, a halo mass with 1.5 h^{-1} Mpc to be 4.6×10^{14} h^{-1} $M_\odot$. The mass parameter $\Omega_{\rm cl}$ of the cluster sample is deduced to be $\Omega_{\rm cl} = 0.077$ for the SIS model and $\Omega_{\rm cl} = 0.083$ for the NFW model, both of which are higher than the observational value. We argue that the overestimate may be caused by the cluster environment and the line-of-sight effect. By comparing, we find that the systematic errors in $\Omega_{\rm cl}$ in Croom & Shanks (1999) and Myers et al. (2003) are much reduced.

References

Abazajian K., Adelman-McCarthy Jennifer K., Agüeros Marcel A. et al., 2004, AJ, 128, 502
Abell G. O., 1958, ApJS, 3, 211
Bahcall N. A., et al. 2003, ApJS, 148, 243
Bartelmann M., Schneider P., 1992, A&A, 259, 413
Bartelmann M., Schneider P., 1993, A&A, 271, 421
Bartelmann M., Schneider P., 1994, A&A, 284, 1
Bartsch A., Schneider P., Bartelmann M., 1997, A&A, 319, 375
Benítez N., Sanz J. L., Martínez-González E., 2001, MNRAS, 320, 241

Boyle B. J., Fong R., Shanks T., 1988, MNRAS, 231, 897
Brainerd T. G., Blandford R. D., Smail I., 1996, ApJ, 466, 623
Cen R., Ostriker J. P., 1999, ApJ, 514, 1
Chu Y. Q., Zhu X. F., 1984, Chin. Astron. Astrophys., 8, 238
Colberg J. M., White S. D. M., Jenkins A., Pearce F. R., 1999, MNRAS, 308, 593
Colín P., Klypin A. A., Kravtsov A. V., Khokhlov A. M., 1999, ApJ, 523, 32
Contaldi C. R., Hoekstra H., Lewis A., 2003, Physical Review Letters, 90, 221303
Croom S. M., Shanks T., 1999, MNRAS, 307, L17
Croom S. M., Smith R. J., Boyle B. J. et al., 2004, MNRAS, 349, 1397
Eisenstein D. J., et al., 2001, AJ, 122, 2267
Fan Z., Chiueh T., 2000, ApJ, 538, 1
Fugmann W., 1988, A&A, 204, 73
Fugmann W., 1990, A&A, 240, 11
Fukugita M., Shimasaku K., Ichikawa T., 1995, PASP, 107, 945
Fukugita M., Hogan C. J., Peebles P. J. E., 1998, ApJ, 503, 518
Gaztañaga E., 2003, ApJ, 589, 82
Goto T., et al., 2002, AJ, 123, 1807
Griffiths R. E., Casertano S., Im M. et al., 1996, MNRAS, 282, 1159
Hoekstra H., Yee H. K. C., Gladders M. D., 2001a, ApJ, 558, L11
Hoekstra H., et al., 2001b, ApJ, 548, L5
Hoekstra H., 2003, IAU Symposium, 216
Maoz D., Rix H. W., 1993, ApJ, 416, 425
Maoz D., Rix H. W., Gal-Yam A., Gould A., 1997, ApJ, 486, 75
Martínez H. J., Merchán M. E., Valotto C. A. et al., 1999, ApJ, 514, 558
Mo H. J., Peacock J. A., Xia X. Y., 1993, MNRAS, 260, 121
Myers A. D., Outram P. J., Shanks T. et al., 2003, MNRAS, 342, 467
Myers A. D., Outram P. J., Shanks T. et al., 2005, MNRAS, 359, 741
Navarro J. F., Frenk C. S., White S. D. M., 1995, MNRAS, 275, 720
Navarro J. F., Frenk C. S., White S. D. M., 1996, ApJ, 462, 563
Navarro J. F., Frenk C. S., White S. D. M., 1997, ApJ, 490, 493
Norman D. J., Impey C. D., 1999, AJ, 118, 613
Norman D. J., Impey C. D., 2001, AJ, 121, 2392
Peebles P. J. E., 1980, The Large-scale Structure of the Universe, Princeton University Press
Richards G. T., et al., 2002, AJ, 123, 2945
Richards G. T., et al., 2004, ApJS, 155, 257
Richards G. T., et al., 2005, MNRAS, 477
Rodrigues-Williams L. L., Hogan C. J., 1994, AJ, 107, 451
Schneider P., Ehlers J., Falco E. E., 1992, Gravitational Lenses, Berlin: Springer
Schneider P., 1993, A&A, 279, 1
Scranton R., et al., 2005, ApJ, 633, 589
Seldner M., Peebles P. J. E., 1979, ApJ, 227, 30
Strauss M. A., et al., 2002, AJ, 124, 1810
Struble M. F., Rood H. J., 1999, ApJS, 125, 35
Tang S. M., Zhang S. N., 2005, Chin. J. Astron. Astrophys. (ChJAA), 5(S), 147
Tegmark M., et al., 2004, Phys. Rev. D, 69, 103501
Turner E. L., Ostriker J. P., Gott J. R., 1984, ApJ, 284, 1
Vanden Berk D. E., et al., 2005, AJ, 129, 2047
Webster R. L., Hewett P. C., Harding M. E., Wegner G. A., 1988, Nature, 336, 358
Williams L. L. R., Irwin M., 1998, MNRAS, 298, 378
Wu X. P., Han J., 1995, MNRAS, 272, 705
Wu X. P., Fang L. Z., 1996, ApJ, 461, L5
Yang Y. B, Yuan Q. R., Wen Z. L. et al., 2005, ApJ, submitted
Young P., Gunn J. E., Oke J. B. et al., 1980, ApJ, 241, 507